Quasiparticle energies and excitonic effects of the two-dimensional carbon allotrope graphdiyne: Theory and experiment

Guangfu Luo, Xuemin Qian, Huibiao Liu, Rui Qin, Jing Zhou, Linze Li, Zhengxiang Gao, Enge Wang, Wai-Ning Mei, Jing Lu, Yuliang Li, and Shigeru Nagase

Phys. Rev. B **84**, 075439 — Published 8 August 2011

DOI: 10.1103/PhysRevB.84.075439

Quasiparticle energies and excitonic effects of graphdiyne: Theory and experiment

Guangfu Luo,[1,2] Xuemin Qian,[3] Huibiao Liu,[3] Rui Qin,[1] Jing Zhou,[1] Linze Li,[1] Zhengxiang Gao,[1] Enge Wang,[1] Wai-Ning Mei,[4] Jing Lu,[1,*] Yuliang Li,[3*] and Shigeru Nagase[2,*]

[1]State Key Laboratory for Mesoscopic Physics and Department of Physics, Peking University, Beijing 100871, P. R. China

[2]Department of Theoretical and Computational Molecular Science, Institute for Molecular Science, Okazaki 444-8585, Japan

[3]Key Laboratory of Organic Solids, Beijing National Laboratory for Molecular Sciences, Institute of Chemistry, Chinese Academy of Sciences, Beijing 100190, P. R. China

[4]Department of Physics, University of Nebraska at Omaha, Omaha, Nebraska 68182-0266

* Corresponding author. E–mail: jinglu@pku.edu.cn, ylli@iccas.ac.cn, nagase@ims.ac.jp

ABSTRACT

We report the electronic structure and optical properties of the recently synthesized stable two-dimensional carbon allotrope—graphdiyne based on first-principles calculations and experimental optical spectrum. Due to the enhanced Coulomb interaction in reduced dimensionality, the band gap of graphdiyne increases to 1.10 eV within the *GW* many-body theory from a 0.44 eV within the density functional theory. The optical absorption is dominated by excitonic effects with remarkable electron-hole binding energy of over 0.55 eV within the *GW*-Bethe Salpeter equation calculation. Experimental optical absorption of graphdiyne films is performed and comparison with the theoretical calculations is analyzed in detail.

PACS numbers: 73.22.-f, 78.67.-n, 71.35.-y, 73.63.-b

Introduction

Because of the three hybridization forms (*sp*, sp^2, and sp^3), carbon can form a variety of allotropes, such as diamond and graphite in nature. From zero–dimensional (0D) fullerene, quasi–one–dimensional (1D) carbon nanotube to two–dimensional (2D) graphene,[1] every synthesis of such novel stable carbon allotrope stimulates extensive theoretical and experimental studies. Graphene consists of extended network of sp^2 hybridized carbon atom and is featured by an extremely high carrier mobility (7×10^4 $cm^2\ V^{-1}\ s^{-1}$ for ferroelectric–gate–oxide supported sample[2] and 1.2×10^5 $cm^2\ V^{-1}\ s^{-1}$ for suspended sample[3] around room temperature, which are 1–2 orders of magnitude larger than that of Si). Pristine graphene, however, cannot be used for effective field effect transistor (FET) operating at room temperature because of its zero band gap.[4, 5] Hence opening a band gap in graphene turns out to be one of the most important and urgent topics in the graphene research community.[6]

Graphyne, a layer compound containing both *sp* and sp^2 hybridized carbon atoms, was proposed theoretically in 1987 as another novel 2D carbon allotrope.[7] The name ‘‘graphyne’’ was coined because of its structure can be constructed by replacing one-third of the carbon−carbon bonds in graphene with acetylenic linkages (−C≡C−). Various substructures of one member of graphyne family—graphdiyne (containing two acetylenic linkages between carbon hexagons, see Figure 1(a)) have been synthesized.[8-11] Only until recently, crystalline film of graphdiyne has been synthesized by Li *et al*. with an area up to several cm^2 in a facile way on the surface of Cu foil.[12, 13] Graphdiyne is found experimentally to be high chemically stable because the dialkyne between the benzene rings is very stable. The electronic structure of graphdiyne is characterized by a direct band gap of 0.53 eV and small carrier effective mass ($0.073m_0$ for electron and $0.075m_0$ for hole, where m_0 is the free electron mass) from the early density functional theory (DFT) calculation.[14] A new theoretical calculation based on DFT coupled with Boltzmann transport equation further predicts that the electron mobility of graphdiyne can reach up to the order of 10^5 $cm^2\ V^{-1}\ s^{-1}$ at room temperature.[15] With these distinguished properties, graphdiyne can easily be used as an effective room–temperature FET

without resorting to an external electrical field or a structural modification to open a band gap as that is required for graphene FET.

Electronic structure and optical absorption are two fundamental properties of material, and an accurate description of them is the basis for further study of graphdiyne. It has been well established that the many–body effects (self–energy correction and electron–hole interaction) on the electronic structure and optical absorption are greatly enhanced in low–dimensional system, such as quasi–1D nanowires,[16] nanotubes,[17, 18] nanoribbons,[19-21] and 2D monolayers[18, 22-24] owing to the reduced Coulomb screening and geometrical confinement. Thus we expect to find out crucial influences of many–body effects on the electronic structure and optical absorption of graphdiyne too. In this article, we calculate the quasiparticle energies and optical absorption of graphdiyne, measure the optical absorption of graphdiyne films, and observe good agreement between the theoretical and experimental spectra, which demonstrates significant many-body effects in this 2D material.

Theories and Methods

In our calculations, we first compute the wavefunctions of the valence bands and a large number of conduction bands by using DFT within the local density approximation (LDA). A plane–wave energy cutoff of 600 eV is used together with norm–conserving pseudopotentials,[25] and the Brillouin zone is sampled with a 12×12×1 Monkhorst–Pack grid. The structure is fully optimized till the force on each atom is less than 10^{-5} eV/Å. Second, the quasiparticle energies E_{nk} are calculated through the following quasiparticle Schrödinger equation with the self–energy Σ acquired from the *GW* approximation.[26]

$$[-\frac{\nabla^2}{2}+V_{ion}+V_{Hartree}+\sum(E_{nk})]\psi_{nk}=E_{nk}\psi_{nk} \quad (1)$$

The Green function and Coulomb screening are constructed from the LDA results,[27] and the plasmon–pole model is used for the screening computation. We carry out the *GW* calculation in a non–self–consistent way, namely the G_0W_0 approximation, and obtain quasiparticle band gap converged within 0.05 eV.[28] Third, electron–hole interaction (excitonic effects) and macroscopic dielectric function are calculated by solving the Bethe–Salpeter equation (BSE),[26, 29]

$$(E_{ck} - E_{vk})A^S_{vck} + \sum_{k'v'c'} \langle vck \mid K^{eh} \mid v'c'k' \rangle A^s_{vck} = \Omega^S A^S_{vck} \quad (2)$$

where A^s_{vck} and Ω^S is the exciton amplitude and energy, respectively; K^{eh} is the electron–hole interaction kernel; $|ck\rangle$ is the quasielectron state and $|vk\rangle$ the quasihole state. The *k*-point sampling is doubled to 24×24×1 and 10 valence bands and 10 conduction bands are included in the optical absorption spectra.[28] To eliminate the mirror effect between neighbor supercells, we separate the layers by 15 Å and truncate the Coulomb force[30] in the out–of–plane direction for both the *GW* and BSE calculations. All calculations are conducted by combing the ABINIT and YAMBO codes.[31, 32]

In our experiment, graphdiyne films are primarily grown on the surface of Cu foil as thoroughly described in a previous report.[12] Then the films are removed from the Cu foils by etching in an aqueous solution of iron nitrate (0.1 mol/L) for 12 hours. A quartz glass substrate is brought into contact with the graphdiyne film and pulled out from the solution, when the copper foil is completely dissolved. After that, the graphdiyne film on the quartz glass substrate is washed by deionized water for several times and dried at 150 °C under vacuum. Finally, the samples are used for measurement of Ultra violet–visible–near infrared (UV–VIS–NIR) spectrum with a V–570 UV–VIS–NIR spectrophotometer (JASCO, Japan).

Results and Discussions

First in Figure 1(b), we compare the band structure and density of states of graphdiyne calculated at the LDA level and *GW* level that take account of the quasiparticle effects. The self–energy correction is apparent. Namely, the band gap is 0.44 eV at the LDA level (0.51 and 0.88 eV are obtained by using the TPSS and HSE hybrid functionals,[33] respectively) and noticeably increases to 1.10 eV at the *GW* level. Such a 1.5 times quasiparticle correction is the consequence of the enhanced Coulomb interaction in reduced dimensionality. It is comparable with that (143%) in the armchair graphene nanoribbon with 10 carbon dimer chains in width (10-AGNR)[20, 34] and that (192%) in the (8,0) single–walled carbon nanotube (SWCNT).[17] All the self–energy corrections in the aforementioned low–dimensional systems are much larger than that (41%) in bulk diamond.[35] The quasiparticle band gap of graphdiyne is quite close to that of Si (1.17 and 1.29 eV for experimental and theoretical value,

respectively[35]), but superior to Si, the band gap of graphdiyne is direct and thus leads to higher luminescence efficiency. Therefore, graphdiyne appears quite suitable for both semiconductor and optoelectronic devices. As shown in Figure 1(c), the quasiparticle correction both to the conduction and valence bands can be clearly classified into two groups according to the correction magnitude, implying that there is no simple "scissor rule" to obtain the quasiparticle band structure from that of the LDA.

The conduction band minimum (CBM) and valence band maximum (VBM) are doubly degenerated at the Γ point. At the LDA level, the effective mass of electron is $m_e^{\Gamma K}$ = 0.069/0.087m_0 and $m_e^{\Gamma M}$ = 0.068/0.084m_0 along the Γ→*K* and Γ→*M* direction, respectively, and the effective mass of hole is $m_h^{\Gamma K}$ = 0.071/0.089m_0 and $m_h^{\Gamma M}$ = 0.070/0.085m_0. The early LDA calculation reported similar values of m_e = 0.073m_0 and m_h = 0.075m_0.[14] Quasiparticle effects slightly decrease the effective masses by 8%. Such small effective masses in graphdiyne are close to the theoretical value (m_e = 0.03m_0) in bilayer graphene,[36] the experimental values (m_e = 0.06m_0 and m_h = 0.03m_0 for light hole and 0.1m_0 for heavy hole) in few–layer graphene,[37] and the theoretical value (0.057~0.079m_0) in graphene nanoribbons.[38] Hence a rather high carrier mobility in graphdiyne is expected. Actually, a recent theoretical calculation has indeed proved its carrier mobility to be comparable to that in graphene.[15]

In Figure 2, the imaginary part of polarizability[39] at the LDA level with random–phase approximation (RPA), the *GW* level with RPA, and finally BSE level are compared, where the light is polarized along the *x* direction. Among them, the optical absorption spectrum at the LDA+RPA level is characterized by three peaks centered on 0.66, 1.77, and 4.02 eV. The first peak originates from transitions around the band gap and the two latter from transitions around the Van Hove singularities at the *M* and *K* point, respectively, as indicated in Figure 1(b). Quasiparticle effects overall shift the spectrum to higher energy and the three peaks respectively move to 1.18, 2.50, and 4.93 eV. The spectrum intensity at the *GW*+RPA level slightly decreases in the meantime. When the electron–hole interactions are included, however, the entire spectrum is pushed back with the main peaks sitting at 0.74, 1.75, and

3.99 eV, respectively. Although the positions of the three peaks are close to those of the LDA+RPA spectrum, the intensity of BSE spectrum is largely redistributed—especially the lowest energy peak is greatly enhanced, a similar feature also observed in other systems like graphane.[24]

Below the quasiparticle band gap (1.10 eV), the lowest excitons locate at the middle of the band gap with an exciton binding energy of 0.55 eV and is actually fourfold degenerate: two are bright and two are dark. These excitons correspond to the transitions from the VBM to CBM, and group theory analyses[28] show that the wavefunctions of the VBM (ψ_{VBM}) and CBM (φ_{CBM}) belong to the doubly degenerate $E_{1\mathrm{g}}$ and $E_{2\mathrm{u}}$ symmetry, respectively. In the context of dipole approximation, we find two dominant transition matrix elements, $\left\langle \psi_{\mathrm{VBM}}^{E_{1g}^{(1)}} \mid x \mid \phi_{\mathrm{CBM}}^{E_{2u}^{(1)}} \right\rangle$ and $\left\langle \psi_{\mathrm{VBM}}^{E_{1g}^{(2)}} \mid x \mid \phi_{\mathrm{CBM}}^{E_{2u}^{(2)}} \right\rangle$, and two negligible ones, $\left\langle \psi_{\mathrm{VBM}}^{E_{1g}^{(1)}} \mid x \mid \phi_{\mathrm{CBM}}^{E_{2u}^{(2)}} \right\rangle$ and $\left\langle \psi_{\mathrm{VBM}}^{E_{1g}^{(2)}} \mid x \mid \phi_{\mathrm{CBM}}^{E_{2u}^{(1)}} \right\rangle$, in x polarization (similar for y polarization), but none important in z polarization. Thus there are two bright and two dark excitons in either x or y direction but all dark in z direction. Detailed analyses[28] of all the major excitonic peaks reveal that the excitonic spectrum is primarily contributed by several bands around the Fermi level, and the electron–hole binding energy ranges from 0.55 to 1.17 eV in the energy range we considered, which is comparable to that in graphene (0.60 eV),[23] zigzag graphene nanoribbons (0.67 eV for 8-ZGNR),[21] and semiconducting SWCNTs (~1.00 eV for the (8,0) tube).[17] There are two reasons for the large exciton binding energy in graphdiyne, namely the reduced screening and the quantum confinement effects in 2D system that allow for a lager overlap between the electron and hole wavefunctions. Nevertheless, this exciton binding energy is still smaller than the 1.6 eV in graphane and 2.1 eV in BN sheet, because the latter materials have a much larger quasiparticle band gap of 5.4 and 7.8 eV, respectively[18, 24] and thus less Coulomb screening.

In Figure 3, we show the electron density of the lowest doubly degenerate bright excitons (A_1 and A_2) while fixing the hole (yellow spot) at the density maximum of the π_z orbitals. In both cases, the excitons are tightly bound to the graphdiyne plane, while in graphane the exciton is separated from the carbon atom network.[24] We find the radius of the excitons to be ~7.4 Å, several times smaller than those in the quasi–1D silicon nanowires and SWCNTs[16, 17]

but still larger than the C–C bond length. Due to the significant spatial extent and large binding energy, we deduce that the excitons in graphdiyne have both the Wannier–Mott and Frenkel exciton characteristics.

We measure the optical absorbance of graphdiyne film from NIR to UV energy range. A smooth cubic polynomial is used to subtract the experimental background (Figure 4). The observed absorbance is compared with the theoretical spectra[39] at the LDA+RPA (Figure 5), *GW*+RPA and BSE (Figure 6) levels. Compared with the other two ones, the BSE level gives a result that most matches the experiment: three absorption peaks in experiment, 0.56, 0.89, and 1.79 eV, correspond to the BSE excitonic peaks at 0.75, 1.00, and 1.82 eV, respectively. A strong depression of absorption is found between 2 and 3.5 eV in both profiles. We note that the positions of the first two measured peaks are 0.19 and 0.11 eV lower, respectively, than the BSE prediction. Such a difference is not surprising in view of the fact that the experimental sample is graphdiyne film with interlayer van der Waals interaction, which has known to influence the position of excitonic peak due to the reduced Coulomb interaction with increasing dimensionality. For instance, from hexagonal BN 2D sheet to 3D bulk, the interlayer van der Waals force redshifts the first absorption peak by 0.18 eV,[18] and a similar 0.10 eV redshift is also observed for the direct-band-gap related peak in hexagonal MoS_2.[40] Given the similar dimensionality and the similar (0.10–0.19 eV) redshift for the three systems, the first two observed and calculated peaks agree well in graphdiyne. A separation of graphdiyne monolayer in the future will allow a direct comparison between the BSE and measured absorbances.

Conclusions

Due to the low–dimensionality, we find that the many–body effects significantly modify the electronic structure and optical absorption of the newly synthesized 2D carbon allotrope—graphdiyne. It possesses a direct quasiparticle band gap of 1.10 eV, which is much larger than that calculated from LDA. The excitons have large binding energy of over 0.55 eV and show both Wannier–Mott and Frenkel exciton characteristics. The theoretical monolayer graphdiyne absorbance basically agrees with our measurement on film. In addition, graphdiyne has a very large in–plane Young's modulus of ~412 GPa,[28] a value as large as that

of the silicon carbide (~450 GPa) and ~40% of that in graphene and diamond (~1100 GPa). Combining all these properties, we advocate that graphdiyne is a superb contender for nanoscale semiconductor and optoelectronic device.

Acknowledgements. This work was supported by the NSFC (Grant Nos. 10774003, 21031006, 10874187, and 20873155), National 973 Projects (No. 2007CB936200, MOST of China), Program for New Century Excellent Talents in University of MOE, National Foundation for Fostering Talents of Basic Science (No. J0630311) of China, Grant–in–Aid for Next Generation Super Computing Project (Nanoscience Program) and Specially Promoted Research from the MEXT in Japan, and Nebraska Research Initiative and DOE DE-EE0003174 in United States.

References and Notes

[1]A. K. Geim and K. S. Novoselov, Nat. Mater. **6**, 183 (2007).

[2]X. Hong, A. Posadas, K. Zou, C. H. Ahn, and J. Zhu, Phys. Rev. Lett. **102**, 136808 (2009).

[3]K. I. Bolotin, K. J. Sikes, J. Hone, H. L. Stormer, and P. Kim, Phys. Rev. Lett. **101**, 096802 (2008).

[4]M. Freitag, Nat. Nanotechnol. **3**, 455 (2008).

[5]Y. Sui and J. Appenzeller, Nano Lett. **9**, 2973 (2009).

[6]S. Y. Zhou, G. H. Gweon, A. V. Fedorov, P. N. First, W. A. De Heer, D. H. Lee, F. Guinea, A. H. C. Neto, and A. Lanzara, Nat. Mater. **6**, 770 (2007).

[7]R. H. Baughman, H. Eckhardt, and M. Kertesz, J. Chem. Phys. **87**, 6687 (1987).

[8]W. B. Wan and M. M. Haley, J. Org. Chem. **66**, 3893 (2001).

[9]J. A. Marsden and M. M. Haley, J. Org. Chem. **70**, 10213 (2005).

[10]Q. Zhou, P. J. Carroll, and T. M. Swager, J. Org. Chem. **59**, 1294 (1994).

[11]M. M. Haley, M. L. Bell, J. J. English, C. A. Johnson, and T. J. R. Weakley, J. Am. Chem. Soc. **119**, 2956 (1997).

[12]G. X. Li, Y. L. Li, H. B. Liu, Y. B. Guo, Y. J. Li, and D. B. Zhu, Chem. Commun. **46**, 3256 (2010).

[13]H. B. Liu, J. L. Xu, Y. J. Li, and Y. L. Li, Acc. Chem. Res. **43**, 1496 (2010).

[14]N. Narita, S. Nagai, S. Suzuki, and K. Nakao, Phys. Rev. B **58**, 11009 (1998).

[15]M. Q. Long, L. Tang, D. Wang, Y. L. Li, and Z. G. Shuai, ACS Nano **5**, 2593 (2011).

[16]L. Yang, C. D. Spataru, S. G. Louie, and M. Y. Chou, Phys. Rev. B **75**, 201304 (2007).

[17]C. D. Spataru, S. Ismail-Beigi, L. X. Benedict, and S. G. Louie, Phys. Rev. Lett. **92**, 077402 (2004).

[18]L. Wirtz, A. Marini, and A. Rubio, Phys. Rev. Lett. **96**, 126104 (2006).

[19]L. Yang, M. L. Cohen, and S. G. Louie, Nano Lett. **7**, 3112 (2007).

[20]D. Prezzi, D. Varsano, A. Ruini, A. Marini, and E. Molinari, Phys. Rev. B **77**, 041404 (2008).

[21]L. Yang, M. L. Cohen, and S. G. Louie, Phys. Rev. Lett. **101**, 186401 (2008).

[22]P. E. Trevisanutto, C. Giorgetti, L. Reining, M. Ladisa, and V. Olevano, Phys. Rev. Lett. **101**, 226405 (2008).

[23]L. Yang, J. Deslippe, C. H. Park, M. L. Cohen, and S. G. Louie, Phys. Rev. Lett. **103**, 186802 (2009).

[24]P. Cudazzo, C. Attaccalite, I. V. Tokatly, and A. Rubio, Phys. Rev. Lett. **104**, 226804 (2010).

[25]N. Troullier and J. L. Martins, Phys. Rev. B **43**, 1993 (1991).

[26]G. Onida, L. Reining, and A. Rubio, Rev. Mod. Phys. **74**, 601 (2002).

[27]F. Bruneval and X. Gonze, Phys. Rev. B **78**, 085125 (2008).

[28]See supplementary material for the convergence tests of the *GW* and BSE calculations, group theory analyses, comparison of the major absorption peak positions among all three theoretical levels and experiments, and explanations on the strain calculation for graphdiyne.

[29]M. Rohlfing and S. G. Louie, Phys. Rev. B **62**, 4927 (2000).

[30]C. A. Rozzi, D. Varsano, A. Marini, E. K. U. Gross, and A. Rubio, Phys. Rev. B **73**, 205119 (2006).

[31]X. Gonze, et al., Z. Kristall. **220**, 558 (2005).

[32]A. Marini, C. Hogan, M. Gruning, and D. Varsano, Comput. Phys. Commun. **180**, 1392 (2009).

[33]M. J. Frisch, et al., (Gaussian, Inc., Wallingford CT, 2009).

[34]L. Yang, C. H. Park, Y. W. Son, M. L. Cohen, and S. G. Louie, Phys. Rev. Lett. **99**, 186801 (2007).

[35]M. S. Hybertsen and S. G. Louie, Phys. Rev. B **34**, 5390 (1986).

[36]M. Koshino and T. Ando, Phys. Rev. B **73**, 245403 (2006).

[37]K. S. Novoselov, A. K. Geim, S. V. Morozov, D. Jiang, Y. Zhang, S. V. Dubonos, I. V. Grigorieva, and A. A. Firsov, Science **306**, 666 (2004).

[38]M. Q. Long, L. Tang, D. Wang, L. J. Wang, and Z. G. Shuai, J. Am. Chem. Soc. **131**, 17728 (2009).

[39]Polarizability in the supercell model of a 2D system is defined as $\alpha = d(\varepsilon-1)/4\pi$, where d is the layer distance and ε the macroscopic dielectric function. The absorbance is defined as $A = \mathrm{Im}(\alpha)4\pi\omega/c = \mathrm{Im}(\varepsilon)d\omega/c$.

[40]K. F. Mak, C. Lee, J. Hone, J. Shan, and T. F. Heinz, Phys. Rev. Lett. **105**, 136805 (2010).

Figure Captions

FIG. 1 (Color online). (a) Geometrical structure, unit cell (red dashed diamond), coordinate bases, first Brillouin zone (green hexagon) of graphdiyne. The structure possess the D_{6h}^{1} space group and a optimized unit cell length of 9.42 Å. (b) Band structures and density of states (DOS) of graphdiyne at the LDA and *GW* levels. Optical transitions between the first two Van Hove singularities are indicated. (c) Quasiparticle correction as a function of the LDA energy in graphdiyne. The linear fit of the data are plotted in red lines.

FIG. 2 (Color online). Imaginary part of polarizability of graphdiyne calculated using the LDA+RPA (black solid line), *GW*+RPA (green dotted line), and BSE (red solid line) approaches. A Gaussian smearing of 0.1 eV is used to broaden all the theoretical spectra.

FIG. 3 (Color online). Top and side views of electron densities of the lowest doubly degenerate bright excitons: A_1 $\left(\psi_{\mathrm{VBM}}^{E_{1g}^{(1)}} \rightarrow \varphi_{\mathrm{CBM}}^{E_{2u}^{(1)}}\right)$ and A_2 $\left(\psi_{\mathrm{VBM}}^{E_{1g}^{(2)}} \rightarrow \varphi_{\mathrm{CBM}}^{E_{2u}^{(2)}}\right)$ in the upper and lower panels, respectively. The hole is fixed at the yellow spot, and the green arrow indicates the direction of the side view.

FIG. 4 (Color online). Raw experimental absorbance (blue circle) of graphdiyne film and cubic polynomial fit (pink solid line) for its background.

FIG. 5 (Color online). Experimental absorbance (blue circle) of graphdiyne film and LDA+RPA absorbance (black solid line) of graphdiyne.

FIG. 6 (Color online). Experimental absorbance (blue circle) of graphdiyne film and theoretical absorbance at the *GW*+RPA (green dotted line) and BSE (red solid line) level of graphdiyne.

Figure 1

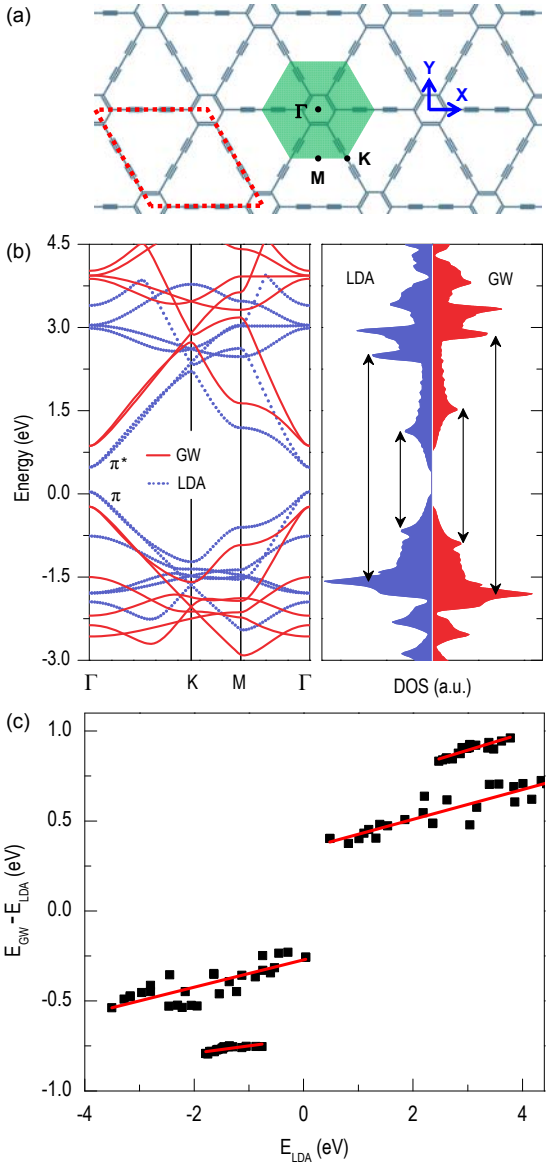
(a)
Γ
K
M
Y
X
(b)
Energy (eV)
4.5
3.0
1.5
0.0
-1.5
-3.0
Γ
K
M
Γ
π*
π
GW
LDA
LDA
GW
DOS (a.u.)
(c)
E_GW - E_LDA (eV)
1.0
0.5
0.0
-0.5
-1.0
-4
-2
0
2
4
E_LDA (eV)

Figure 2

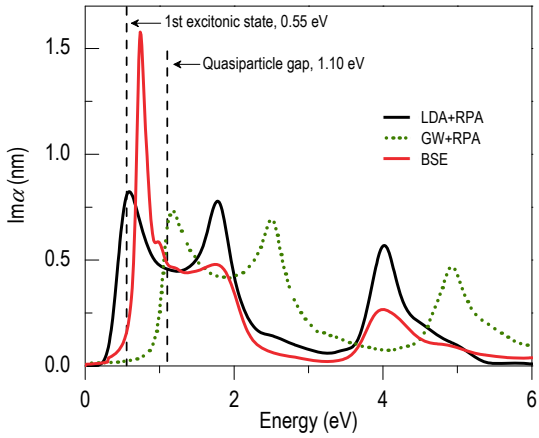
1st excitonic state, 0.55 eV
Quasiparticle gap, 1.10 eV
LDA+RPA
GW+RPA
BSE
Imα (nm)
Energy (eV)
0.0
0.5
1.0
1.5
0
2
4
6

Figure 3

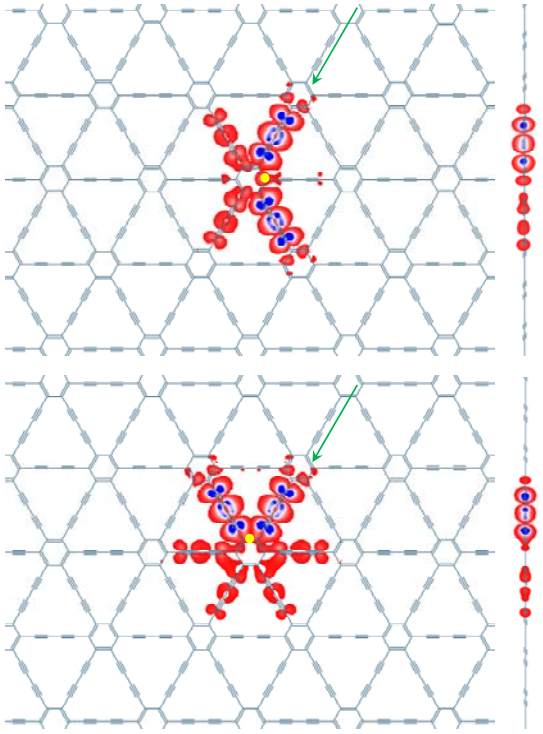

Figure 4

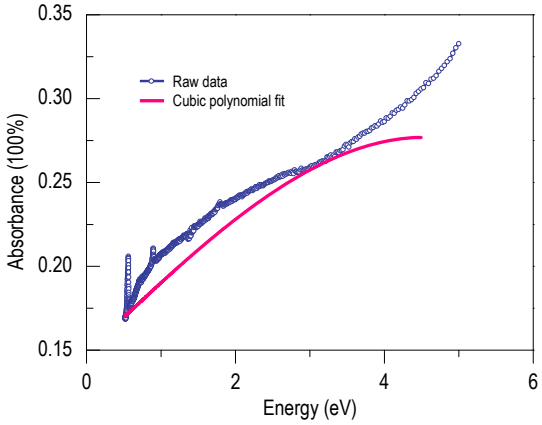
0.35
0.30
0.25
0.20
0.15
Absorbance (100%)
Raw data
Cubic polynomial fit
0
2
4
6
Energy (eV)

Figure 5

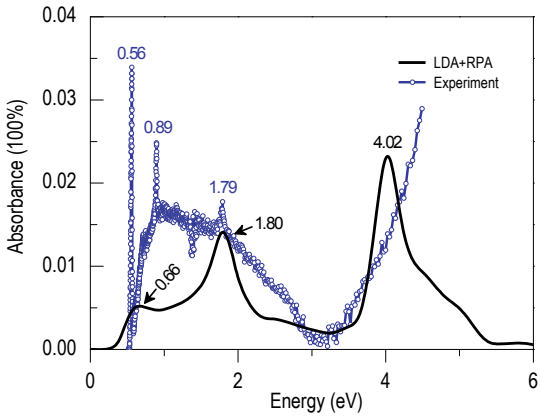
0.04
0.03
0.02
0.01
0.00
Absorbance (100%)
0
2
4
6
Energy (eV)
LDA+RPA
Experiment
0.56
0.89
1.79
1.80
0.66
4.02

Figure 6

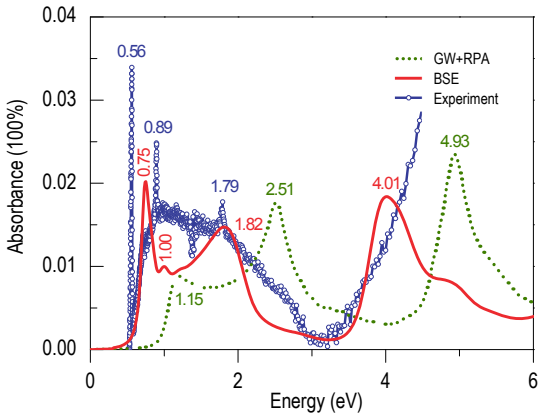
0.04
0.03
0.02
0.01
0.00
Absorbance (100%)
0
2
4
6
Energy (eV)
GW+RPA
BSE
Experiment
0.56
0.89
0.75
1.00
1.79
1.82
2.51
1.15
4.01
4.93